Journal of Materials Chemistry C

PAPER

View Article Online
View Journal | View Issue

Cite this: J. Mater. Chem. C, 2014, 2, 1667

Synthesis and mesomorphism of triphenylene-based dimers with a highly ordered columnar plastic phase†

Yifei Wang, Chunxiu Zhang,* Hao Wu and Jialing Pu

Received 9th October 2013
Accepted 4th December 2013

DOI: 10.1039/c3tc31986e

www.rsc.org/MaterialsC

A series of triphenylene-based discotic dimers have been synthesized, each of the triphenylene nuclei bears five β-OC_4H_9 substituents, which are linked through the remaining β-positions by a flexible $O(CH_2)_nO$ polymethylene chain (n = 2–12). Their chemical structures were confirmed by proton nuclear magnetic resonance spectroscopy, Fourier transform infrared spectroscopy, high-resolution mass spectrometry and elemental analysis. The mesomorphic properties of these compounds were investigated by differential scanning calorimetry, polarizing optical microscopy and X-ray diffraction. It was found that these dimers for which n > 4 formed a highly ordered columnar plastic phase and some of them (n = 6, 7, 10, 11, and 12) exhibited multiple mesophases. This is the first time that the rectangular columnar plastic phase was defined by us as a novel liquid crystal phase of compound **4d** (n = 5). The introduction of a single interconnecting chain between adjacent molecules does not significantly perturb the formation of a columnar plastic phase but enriches the mesophases of discotic molecules and hinders the crystallization; the mesophases of **4e–k** (n = 6–12) can be supercooled into a glass state in which the self-assembly columnar structures are retained.

Introduction

Discotic liquid crystals are an emerging class of organic semiconductors. The discs stack on top of each other and arrange in columnar phases, maximizing the π-orbital overlap between adjacent molecules and thus favouring a one-dimensional charge transport along the column.[1–4] These unique electronic properties together with their solubility make them promising materials for low cost solution processing organic electronic devices.[5–8]

Since D. Haarer's seminal report on the photoconductivity of the discotic liquid crystal hexahexylthiotriphenylene (HTT6), charge carrier transport in columnar liquid crystals has turned into one of the most active fields in organic semiconducting materials.[9–12] Mobilities of the order of 10^{-2} to 10^{-1} $cm^2\ V^{-1}\ s^{-1}$ are reported in columnar mesophases, which are comparable to those of organic single crystals.[2,3] These remarkable high mobilities are generally obtained either from molecules with large aryl cores such as hexabenzocoronenes and phthalocyanines or from the molecules which can form the highly ordered columnar phases, for instance, the helical phase and the columnar plastic phase.[13–19] However, large rigid cores increase the difficulty of synthesis, purification and alignment, which considerably limiting their practical applications. The formation of highly ordered columnar phases seems to offer a perfect strategy for improving applicable materials, since the mobilities exceeding 10^{-3} $cm^2\ V^{-1}\ s^{-1}$ can be easily achieved by simple molecules in their highly ordered columnar phase, such as hexahexylthiotriphenylene (HTT6) and hexabutyloxytriphenylene (HAT4). These molecules are relatively easy to synthesize and also less complex when handling for device fabrication.

A columnar plastic phase is highly appealing as one of the highly ordered phases. It is reported to have a three-dimensional positional order, as in a crystalline state, while maintaining the rotational mobility, thus defined as a columnar plastic phase.[16,17] Besides the three-dimensional order, this phase is very closely related to the normal columnar phase, they share similar character of fluidity and no major differences in structure and dynamics are observed. But the charge mobility of the columnar plastic phase can reach the order of 10^{-2} $cm^2\ V^{-1}\ s^{-1}$ which is about an order of magnitude higher than that of the normal columnar phase.[13,16,17] However, these minor changes can highly affect the packing and transport properties which is still not quite clear. The investigation of the columnar plastic phase will surely lead to further understanding of the self-assembling process as well as the nature of the photoconductivity. Furthermore, the fluidity and high charge mobility of the columnar plastic phase are also two applicable characteristics for being charge transport layers in electronic devices.

Information Recording Materials Lab, Lab of Printing & Packaging Material and Technology, Beijing Institute of Graphic Communication, 102600 Beijing, China. E-mail: zhangchunxiu@bigc.edu.cn; Fax: +86-10-60261108; Tel: +86-10-60261110

† Electronic supplementary information (ESI) available: Experimental data, synthesis, characterization, polarized optical microscopy, and thermal analysis. See DOI: 10.1039/c3tc31986e

To date, there are few reports concerning the columnar plastic phase, even molecules exhibiting this phase are rare. The aim of this work is to obtain more model discotic molecules which exhibit a columnar plastic phase and to devise a systematic study on this phase. Triphenylene derivative hexabutyloxytriphenylene (HAT4) which has been frequently reported to demonstrate a columnar plastic phase is chosen as a precursor to form dimers with the flexible linkage $O(CH_2)_nO$.[13] According to the previous studies on hexapentyloxytriphenylene (HAT5) and hexahexyloxytriphenylene (HAT6), a conclusion can be drawn that the order of the columnar phase is independent of the flexible alkyl linkage chain.[20,21] The series of hexabutyloxytriphenylene dimers are therefore anticipated to have a columnar plastic phase.

Results and discussion

Synthesis

The synthesis of the dimers **4a–k** is shown in Scheme 1. Iron(III) chloride mediated oxidative coupling of 1,2-dibutoxy-benzene followed by a reductive methanol workup gave 2,3,6,7,10,11-hexabutyloxytriphenylene.[22] Selective ether cleavage using B-bromocatecholborane gave 2-hydroxy-3,6,7,10,11-pentabutoxy-triphenylene,[23] which was reacted with anhydrous potassium carbonate and 0.5 equiv. of the appropriate α,ω-dibromoalkane in refluxing ethanol to give the dimers **4a–k**.[24]

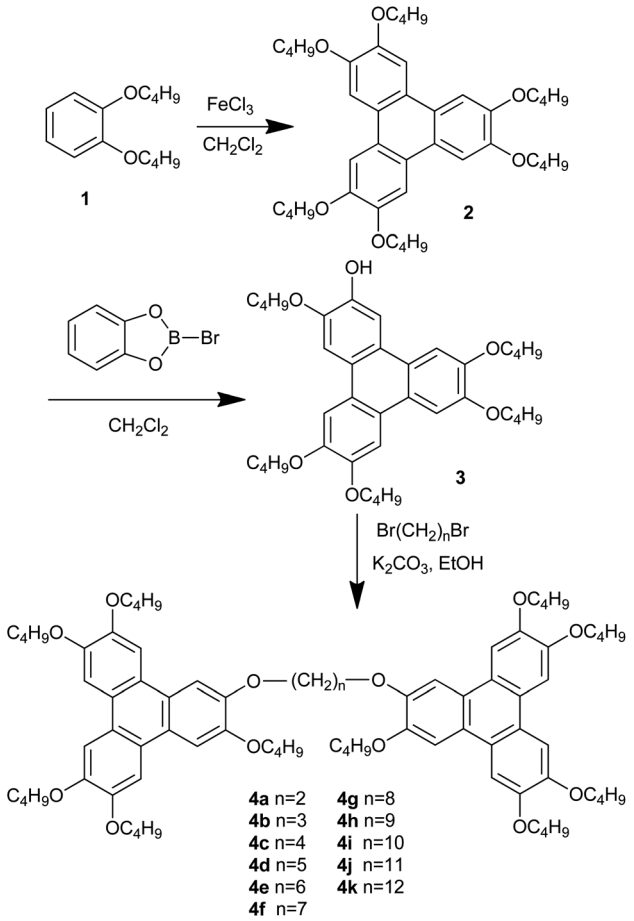

Scheme 1 Synthesis of triphenylene dimers **4a–k**.

Mesomorphism

The phase behaviors of triphenylene dimers **4a–k** were investigated by differential scanning calorimetry (DSC), polarizing optical microscopy (POM) and variable temperature X-ray diffraction (XRD). Compounds **4a–c** did not show liquid crystal behavior while compounds **4d–f** and **4i–k** exhibited two liquid crystal phases and **4g** and **4h** gave a single liquid crystal phase. Phase assignment and transition temperature are summarized in Fig. 1.

In the DSC thermograms of compound **4d**, two endothermic peaks located at 94 °C and 122 °C were observed during the first heating run, corresponding to crystalline phase–mesophase and mesophase–isotropic phase transitions, respectively (Fig. 2). Even though a signature focal conic texture of the columnar phase was observed by POM at 120 °C, the DSC curves of the first cooling run exhibited only one exothermic peak at 79 °C (Fig. 4b).

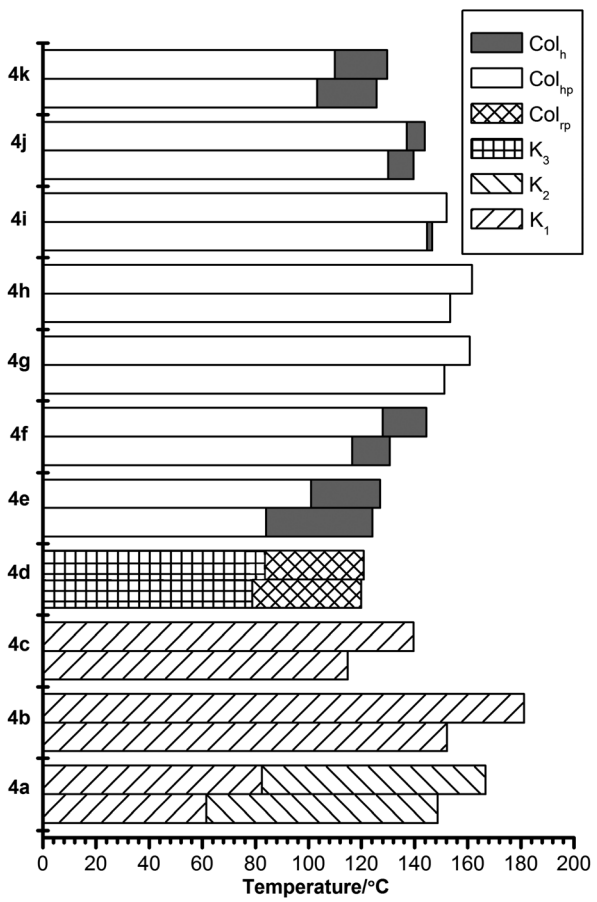

Fig. 1 Graph of phase transition temperatures on heating (above column) and cooling (below column). Transition temperatures are based on the 1st cooling and 2nd heating runs by DSC at 10 °C min^{-1}. Phase assignments of **4a–c** are based on the observation of DSC and POM; **4d–k** are based on XRD (Col_h = hexagonal columnar phase; Col_{hp} = hexagonal columnar plastic phase; Col_{rp} = rectangular columnar plastic phase; K_1, K_2, and K_3 = crystalline phase).

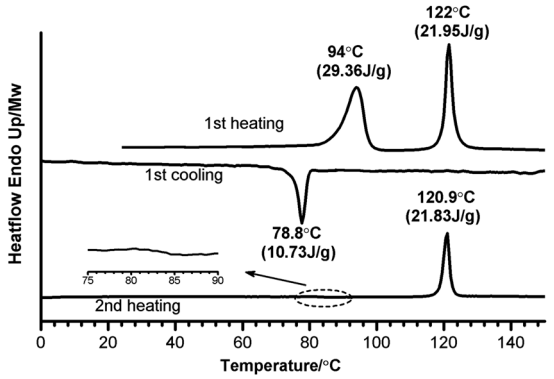

Fig. 2 DSC curves of **4d** with a rate of 10 °C min^{-1}.

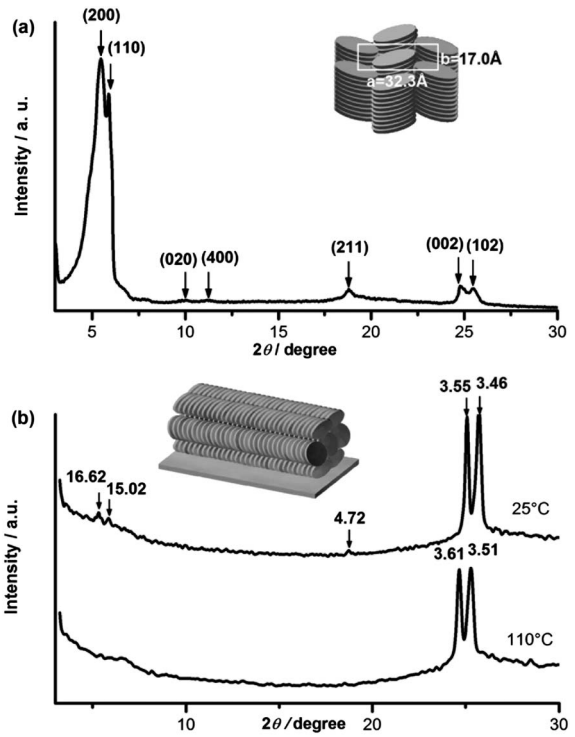

Fig. 3 (a) XRD pattern of **4d** at 120 °C on heating and the supposed structure of the Col_{rp} phase (insert); (b) XRD pattern of **4d** at 110 °C and 25 °C on cooling and the schematic of the edge-on arrangement (insert), the numbers give the corresponding Bragg distances in Å.

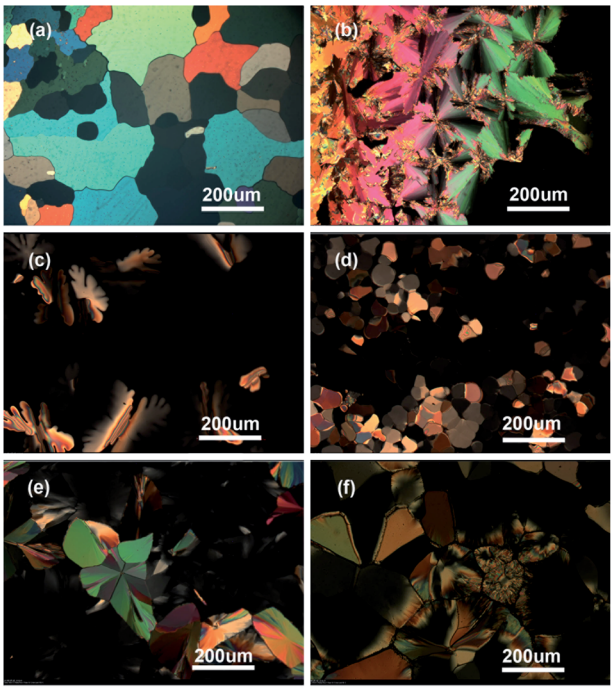

Fig. 4 (a) Mosaic texture for the Col_{hp} phase of HAT4 at 95 °C; (b) focal conic texture for the Col_{rp} phase of **4d** at 90 °C; (c) dendritic texture for the Col_h phase of **4f** at 130 °C; (d) mosaic texture for the Col_{hp} phase of **4f** at 110 °C; (e) mosaic texture for the Col_{hp} phase of **4g** at 150 °C; (f) mosaic texture for the Col_{hp} phase of **4h** at 150 °C (magnification 100×).

This transition was identified as a crystalline transition, since the coexistence of the focal conic texture and small crystalline grains was observed (ESI Fig. 29†). A second order transition which indicated a crystalline phase–mesophase transition was also detected during the second heating run at 84 °C.

A unique X-ray pattern was observed when heating **4d** into its mesophase from unoriented bulk material (Fig. 3a). At larger scattering angles (about $2\theta = 25°$), a doublet reflection was detected, which is a signature of the columnar plastic phase.[16] The smaller scattering angles (about $2\theta = 5°$–$15°$) showed two separate peaks of roughly equal intensity and additional peaks of lower intensity, these peaks were identified as the (200), (110), (020) and (400) reflections of a two dimensional rectangular lattice in which the molecules are tilted with respect to the column axis.[25,26] It was the first report on a rectangular lattice in a columnar plastic phase, according to the previous definition of the rectangular columnar phase, this new phase could be defined as a rectangular columnar plastic phase. The lattice constants a and b were calculated to be $a = 32.3$ Å and $b = 17.0$ Å from the spacings of d_{200} and d_{110} according to eqn (1).[26]

$$1/d_{hkl}^2 = h^2/a^2 + k^2/b^2 \quad (1)$$

XRD patterns obtained from the cooling process showed sharp diffraction in the wide-angle regime with no or minimal peaks in the small-angle regime (Fig. 3b). This type of diffraction pattern indicated an edge-on alignment with discotic columnar axes oriented parallel to the substrate.[27] On gradually decreasing the temperature, no major changes in the XRD pattern were detected nearby phase transition temperature, combined with the former POM observations, it was obvious that rectangular columnar features were largely preserved.

The DSC curves of **4e**, **4f**, **4j** and **4k** all showed two phase transitions on both heating and cooling runs while **4i** only observed two phase transitions in the cooling run (Table 1). The high temperature phases of these compounds were identified as the Col_h phase on the basis of the characteristic dendritic texture observed by POM (Fig. 4c). The texture of **4e** and **4k** did not show any changes when they were cooled to room

Table 1 Phase behaviours of compounds **4e–k**. Transition temperatures and enthalpies were determined by DSC at a scanning rate of 10 °C min^{-1}

	Phase T/°C (ΔH/J g^{-1}) phase[a]	Process
4e	Col_{hp} 81.8(−2.7) Col_h 123.3(−15.4) I	1st cooling
	Col_{hp} 101(5.1) Col_h 127.1(16.4) I	2nd heating
4f	Col_{hp} 116.6(−9.3) Col_h 130.7(−16.6) I	1st cooling
	Col_{hp} 128(8.9) Col_h 134.5(14.7) I	2nd heating
4g	Col_{hp} 151.3(−33.7) I	1st cooling
	Col_{hp} 160.8(33.9) I	2nd heating
4h	Col_{hp} 154.2(−29.3) I	1st cooling
	Col_{hp} 161.7(30.1) I	2nd heating
4i	Col_{hp} 144.8 Col_h 146.7 I	1st cooling
	Col_{hp} 152.1(27) I	2nd heating
4j	Col_{hp} 130.6(−5.7) Col_h 140.8(−16.3) I	1st cooling
	Col_{hp} 137.1 Col_h 143.9 I	2nd heating
4k	Col_{hp} 103.3(−3.2) Col_h 125.8(−15.6) I	1st cooling
	Col_{hp} 110(3.5) Col_h 129.7(13.1) I	2nd heating

[a] Compounds **4e**, **4f** and **4i–k** exhibited two liquid crystal phases.

temperature although there were obvious transitions on their DSC curves of the cooling run.

Phase transitions of **4f**, **4i**, and **4j** were clearly observed by POM, the colours and areas of domain were changed while the birefringence increased, their textures were finally translated into mosaic texture (Fig. 4d),[28] and this typical texture was exactly similar to the texture observed in the hexagonal columnar plastic phase (Col_{hp}) of HAT4 (Fig. 4a).

When heating powder samples into the liquid crystal phase, compound **4e** did not show any available diffraction in the XRD pattern. However, the low temperature phase of compounds **4f** and **4i–k** gave analogous X-ray diffraction patterns, two diffraction peaks in the wide-angle regime indicated a columnar plastic phase, and reflections in the small-angle regime were originated from a hexagonal packing (Table 2).[26] Thus they could be clearly confirmed as a Col_{hp} phase. Their lattice constants a were calculated from the spacings of d_{100} according to eqn (2).[26] Among these compounds, only **4k** showed the characteristic diffraction peaks of Col_h at its high temperature liquid crystal phase on heating (Fig. 5a).

$$1/d_{hk}^2 = 4(h^2 + k^2 + hk)/3a^2 \quad (2)$$

Phase transitions between Col_h and Col_{hp} of **4e**, **4f**, **4j** and **4k** were best observed in the X-ray diffraction patterns obtained on cooling from the isotropic phase, a single diffraction peak of approximately 3.6 Å in the wide-angle in the high temperature phase and the peak split into two reflections in the low temperature phase (Fig. 5b). The XRD pattern of **4i** also failed to show any characteristic diffraction peaks of the Col_h phase on cooling, it may be due to the short temperature range of this phase. An edge-on alignment also obtained when cooling **4e**, **4f**, and **4i–k** from their isotropic phases and their XRD patterns during the cooling process were similar to that of **4d**.

Compounds **4g** and **4h** and compound **4i** which was described above have been reported previously to exhibit a single Col_{hp} phase but neither detailed characterization nor references were conducted.[29] Textures of **4g** and **4h** observed by POM were mosaic texture similar to those mentioned above (Fig. 4e and f). Their DSC traces showed only one peak on both heating and cooling, which were identified as phase transitions between the isotropic phase and the mesophase (Table 1). X-ray patterns detected in their mesophases similar to that of **4i** indicated a Col_{hp} phase.

A general comparison of phase behaviors between these dimers and their monomer HAT4 illustrates the significant role played by the flexible alkyl linkages in promoting their different packing structures.

A two-dimensional rectangular lattice has been frequently reported previously in a normal columnar phase.[26,30,31] It

Table 2 X-ray diffraction data of compounds **4d** and **4f–k** obtained from the heating process

	Temperature/°C	d-Spacing/Å	Miller index (hkl)	Phase (lattice constants)
4d	120	16.17	(200)	Col_{rp} (a = 32.3 Å)
		14.98	(110)	(b = 17.0 Å)
		8.71	(020)	
		7.94	(400)	
		4.71	(211)	
		3.58	(002)	
		3.49	(102)	
4f	125	15.95	(100)	Col_{hp} (a = 18.4 Å)
		9.19	(110)	
		7.96	(200)	
		6.02	(210)	
		4.62	(211)	
		3.61	(002)	
		3.52	(102)	
4g	120	17.45	(100)	Col_{hp} (a = 20.2 Å)
		6.27	(210)	
		5.35	(220)	
		4.74	(211)	
		3.64	(002)	
		3.55	(102)	
4h	150	16.30	(100)	Col_{hp} (a = 18.8 Å)
		9.41	(110)	
		6.15	(210)	
		4.69	(211)	
		3.63	(002)	
		3.53	(102)	
4i	100	16.30	(100)	Col_{hp} (a = 18.8 Å)
		6.17	(210)	
		4.68	(211)	
		3.56	(002)	
		3.48	(102)	
4j	120	16.35	(100)	Col_{hp} (a = 18.9 Å)
		6.19	(210)	
		4.67	(211)	
		3.56	(002)	
		3.48	(102)	
4k	80	16.48	(100)	Col_{hp} (a = 19.0 Å)
		6.41	(210)	
		4.71	(211)	
		3.56	(002)	
		3.48	(102)	
	120	16.56	(100)	Col_h (a = 19.12 Å)
		3.61	(001)	

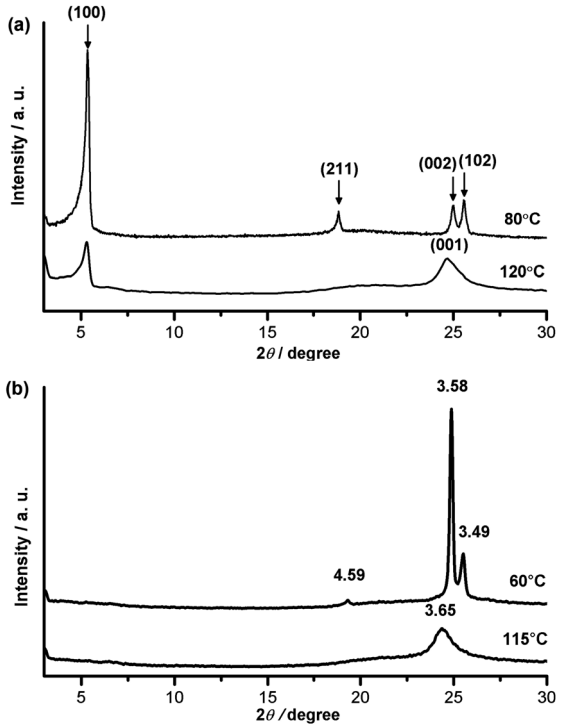

Fig. 5 (a) XRD patterns of **4k** at different temperatures on heating (Col_{hp} at 80 °C and Col_h at 120 °C); (b) XRD patterns of **4e** at different temperatures on cooling (Col_{hp} at 60 °C and Col_h at 115 °C), the numbers give the corresponding Bragg distances in Å.

generally resulted from non-cylindrical columnar cores with elliptical cross-section orthogonal to the long axis of columns.[32] Such elliptical cross-sections are generated either by the molecular shape itself, hindered molecular rotation of non-disklike molecules around the columnar axis,[33–35] or by the tilt of the molecular disks with respect to the columnar axis.[26,32] The short linkage of **4d** makes the conformations in which both triphenylene units are coplanar unlikely. These monomeric units have to tilt with respect to their columnar axis due to the steric crowding when forming the columnar phase *via* self-assembly (Fig. 6). Columns with tilted cores contribute to the presence of elliptical cross-section which is better suited for a rectangular lattice as compared to the hexagonal lattice. It should also be noted that stronger core–core interactions are needed for the formation of a rectangular mesophase than that of the hexagonal mesophase, since the molecules of one column must be tilted in an appropriate way with respect to the molecules of the neighboring columns.[26,36] A strong core–core interaction would be expected in the columnar phase of **4d** for the short bridge chain between two triphenylene nuclei, which also introduces a strain in neighboring columns, thus more likely to meet the requirement for the formation of a rectangular phase. While the exact nature of such an assembly remains ambiguous, it would nonetheless explain the observation that column–column separation of **4d** is slightly smaller than that of HAT4.[19]

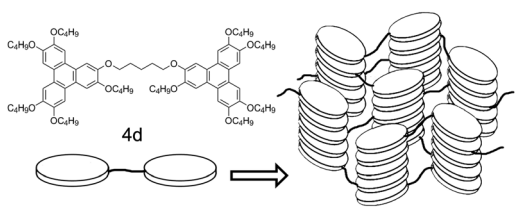

Fig. 6 Schematic illustration of the packing mode of **4d** in the Col_{rp} phase.

The formation of the Col_{hp} phase in **4e–k** can be easily interpreted on the basis of previous studies of dimers.[21,37,38] The linkage in dimers was required to be long enough to afford a low strain bridging between monomeric units. This long spacer allows sufficient orientational freedom of dimer components and the structure of the mesophase can be visualized as columns consisting of stacked separated monomeric units, and thus the mesophases exhibited by **4e–k** are isomorphic with that of the corresponding monomer HAT4. It is also not complicated to understand the absence of mesophase in **4a–c**, since the spacers are too short and no motion is possible.

The occurrence of phase transitions between Col_{hp} and Col_h in **4e**, **4f** and **4i–k** was also of interest, since this type of phase transition was rarely reported and not emerged in dimers before.[17,39] There are no significant differences in rotational dynamics of the triphenylene molecules between the two phases as evidenced by B. Glüsen and coworkers, but the analysis of XRD and thermal expansion coefficients indicated a higher intracolumnar ordering in the Col_{hp} phase rather than in the Col_h phase, hence the charge carrier mobility would be expected to increase in the Col_{hp} phase.[16,17] The multiphase behavior of these dimers would lead to a better understanding of the self-assembly process and also enable us to study the charge transport mechanisms at various phases in one single system.

All these compounds **4e–k** showed no crystal diffraction peaks in XRD patterns at room temperature, the results were agreed with the observations from the DSC and POM. A supercooled columnar plastic phase was confirmed to form at room temperature. It was mentioned above that the columnar plastic phase was a highly ordered phase with a three-dimensional order, and the XRD also showed the shorter stacking distances at the lower temperature. Thus these materials tend to have greater ordering in their supercooled phase, this could be advantageous for room temperature electronic applications, since charge carrier mobility tend to increase with increasing order.

Conclusions

A set of triphenylene-based dimers **4a–k** have been synthesized. Their mesomorphism was fully investigated by DSC, POM and X-ray diffraction. As we had expected, these compounds for which $n > 4$ all formed a highly ordered columnar plastic phase.

In contrast to their monomer HAT4, these dimers exhibited much richer variety columnar phases. A more orderly rectangular columnar plastic phase was formed by **4d**, which is a novel phase that has not been reported before. Analogous phase behaviours were observed in **4e**, **4f** and **4i–k**, they formed a hexagonal columnar plastic phase at low temperature as well as

an ordered hexagonal columnar phase at high temperature. All these columnar plastic phases except that of **4d** could be frozen in a glass state at room temperature. The introduction of a single interconnecting chain between adjacent molecules did not significantly perturb the formation of the columnar plastic phase. Even though no obvious regularity was found between the length of linkage and the phase range of these dimers, the appearance of linkages was thought to enrich the mesophases of discotic molecules and hinder the crystallization.

Besides the doublet diffraction at larger scattering angles in XRD patterns, mosaic texture was also frequently observed in the Col_{hp} phase, this type of texture could therefore be determined as signature texture of this phase. Furthermore, the alignments of these dimers were found to be easily tuned between face-on and edge-on by heat treatment, it has been proved by XRD patterns which indicated a face-on alignment on heating while an edge-on alignment on cooling. This controllable alignment is very important for fabrication of electronic devices such as OLEDs, OPVs and OPCs as well as TFTs.

Since only a few molecules were reported to exhibit the phase transition between the Col_h phase and the Col_{hp} phase, this series of dimers provided more suitable model molecules to discuss the relationship between the order of molecular packing structure and its electronic transportation properties and also facilitate us to investigate the columnar plastic phase in a wider temperature range. They were found to have more advantages for applications since the charge mobility tends to be high in the highly ordered materials. The investigation on photoconductivity of these dimers is proceeding and will be reported in further work.

Experimental

All solvents employed were purchased from Aldrich and used without further purification unless stated otherwise. Column and thin layer chromatography were performed on silica gel 60 (200–300 mesh ASTM) and Silica Gel 60 glass backed sheets, respectively. ^{1}H-NMR spectra were recorded in $CDCl_3$ on Bruker NMR spectrometers (DMX 300 MHz), chemical shifts are given in parts per million (δ) and are referenced from tetramethylsilane (TMS). Multiplicities of the peaks are given as s = singlet, d = doublet, t = triplet, and m = multiplet. Fourier transform infrared spectroscopy (FT-IR) was carried out on a Shimadzu FTIR-8400 spectrometer using KBr pellets. The high-resolution mass spectrum was recorded on a Bruker Apex IV FTMS mass spectrometer. Elemental analysis (C, H) was performed on an Elementar Vario EL CUBE elements analyzer.

Polarising optical microscopy was carried out on a Leica DM4500P microscope equipped with a Linkam TMS94 hot stage. Differential scanning calorimetry was carried out on a Netzsch DSC 200 at a heating and cooling rate of 10 °C min^{-1}. X-ray diffraction studies were conducted on a Bruker D8 Advance diffractometer equipped with a variable temperature controller.

Compounds **1–3** were prepared according to literature procedures and characterized by ^{1}H-NMR and FT-IR;[22,23] compounds **4a–f**, **4j**, and **4k** were synthesised from **3** and the appropriate α,ω-dibromoalkane according to the method reported for compound **4g–i**.[24]

General synthesis of 4a–k

A mixture of 2-hydroxy-3,6,7,10,11-pentabutyloxytriphenylene **3** (500 mg), α,ω-dibromoalkane (0.5 eq.) and anhydrous potassium carbonate (1.0 g) in ethanol (20 ml) was heated under reflux for 72 h. The mixture was cooled to 0 °C, filtered, washed with water (50 ml), and extracted with dichloromethane (2 × 50 ml), the solvent was removed *in vacuo*, and the residue was purified by column chromatography on silica eluting with dichloromethane and finally recrystallized from ethanol to give pure **4a–k**.

1,2-Bis(3′,6′,7′,10′,11′-pentabutyloxytriphenylen-2′-yloxy)-ethane ***4a*** (0.25 g, 49%): TLC R_f: 0.15 (dichloromethane–hexane 2 : 1); (found: C, 75.98; H, 8.87. $C_{78}H_{106}O_{12}$ requires: C, 75.82; H, 8.65%); IR (KBr): ν_{max}/cm^{-1} 1260 (C–O–C); δ_H (300 MHz, $CDCl_3$) 7.81–8.09 (12H, m, ArH), 4.74 (4H, t, OCH_2CH_2O), 4.08–4.22 (20H, m, OCH_2), 1.74–1.96 (20H, m, OCH_2CH_2), 1.43–1.69 (20H, m, $OCH_2CH_2CH_2$), 1.02–1.07 (30H, m, CH_3); HRMS (ESI): calc. m/z 1234.7679 ($C_{78}H_{106}O_{12}$), found m/z 1234.7652 (M)$^+$.

1,3-Bis(3′,6′,7′,10′,11′-pentabutyloxytriphenylen-2′-yloxy)-propane ***4b*** (0.32 g, 63%): TLC R_f: 0.17 (dichloromethane–hexane 2 : 1); (found: C, 75.76; H, 8.71. $C_{79}H_{108}O_{12}$ requires: C, 75.93; H, 8.71%); IR (KBr): ν_{max}/cm^{-1} 1261 (C–O–C); δ_H (300 MHz, $CDCl_3$) 7.81–7.96 (12H, s, ArH), 4.58 (4H, t, OCH_2), 4.13–4.27 (20H, t, OCH_2), 2.57 (2H, m, OCH_2CH_2), 1.79–1.93 (20H, m, OCH_2CH_2), 1.47–1.62 (20H, m, $OCH_2CH_2CH_2$), 0.89–1.07 (30H, m, CH_3); HRMS (ESI): calc. m/z 1248.7835 ($C_{79}H_{108}O_{12}$), found m/z 1248.7822 (M)$^+$.

1,4-Bis(3′,6′,7′,10′,11′-pentabutyloxytriphenylen-2′-yloxy)-butane ***4c*** (0.30 g, 59%): TLC R_f: 0.20 (dichloromethane–hexane 2 : 1); (found: C, 75.90; H, 8.82. $C_{80}H_{110}O_{12}$ requires: C, 76.03; H, 8.77%); IR (KBr): ν_{max}/cm^{-1} 1261 (C–O–C); δ_H (300 MHz, $CDCl_3$) 7.85 (12H, s, ArH), 4.40 (4H, t, OCH_2), 4.18–4.25 (20H, t, OCH_2), 2.26 (4H, m, OCH_2CH_2), 1.82–1.95 (20H, m, OCH_2CH_2), 1.53–1.65 (20H, m, $OCH_2CH_2CH_2$), 1.05 (30H, t, CH_3); HRMS (ESI): calc. m/z 1262.7992 ($C_{80}H_{110}O_{12}$), found m/z 1262.7968 (M)$^+$.

1,5-Bis(3′,6′,7′,10′,11′-pentabutyloxytriphenylen-2′-yloxy)-pentane ***4d*** (0.27 g, 51%): TLC R_f: 0.28 (dichloromethane–hexane 2 : 1); (found: C, 76.14; H, 8.85. $C_{81}H_{112}O_{12}$ requires: C, 76.14; H, 8.84%); IR (KBr): ν_{max}/cm^{-1} 1261 (C–O–C); δ_H (300 MHz, $CDCl_3$) 7.86 (12H, s, ArH), 4.24 (24H, t, OCH_2), 2.11 (4H, t, OCH_2), 1.89–2.08 (22H, m, CH_2), 1.53–1.65 (24H, m, $OCH_2CH_2CH_2$), 1.05 (30H, t, CH_3); HRMS (ESI): calc. m/z 1276.8148 ($C_{81}H_{112}O_{12}$), found m/z 1276.8123 (M)$^+$.

1,6-Bis(3′,6′,7′,10′,11′-pentabutyloxytriphenylen-2′-yloxy)-hexane ***4e*** (0.26 g, 49%): TLC R_f: 0.30 (dichloromethane–hexane 2 : 1); (found: C, 76.17; H, 8.94. $C_{82}H_{114}O_{12}$ requires: C, 76.24; H, 8.90%); IR (KBr): ν_{max}/cm^{-1} 1261 (C–O–C); δ_H (300 MHz, $CDCl_3$) 7.84 (12H, s, ArH), 4.24 (24H, t, OCH_2), 1.92–2.03 (24H, m, OCH_2CH_2), 1.57–1.73 (24H, m, $OCH_2CH_2CH_2$), 1.05 (30H, t, CH_3); HRMS (ESI): calc. m/z 1290.8305 ($C_{82}H_{114}O_{12}$), found m/z 1290.8314 (M)$^+$.

1,7-Bis(3′,6′,7′,10′,11′-pentabutyloxytriphenylen-2′-yloxy)-heptane ***4f*** (0.31 g, 58%): TLC R_f: 0.34 (dichloromethane–hexane 2 : 1); (found: C, 76.26; H, 9.02. $C_{83}H_{116}O_{12}$ requires: C, 76.34; H, 8.95%); IR (KBr): ν_{max}/cm^{-1} 1261 (C–O–C); δ_H (300 MHz, $CDCl_3$) 7.84 (12H,

s, ArH), 4.24 (24H, t, OCH_2), 1.89–1.98 (24H, m, OCH_2CH_2), 1.56–1.68 (26H, m, CH_2), 1.05 (30H, t, CH_3); HRMS (ESI): calc. *m*/*z* 1304.8461 ($C_{83}H_{116}O_{12}$), found *m*/*z* 1304.8436 $(M)^+$.

1,8-Bis(3′,6′,7′,10′,11′-pentabutyloxytriphenylen-2′-yloxy)-octane ***4g*** (0.22 g, 41%): TLC R_f: 0.35 (dichloromethane–hexane 2 : 1); (found: C, 76.38; H, 8.95. $C_{84}H_{118}O_{12}$ requires: C, 76.44; H, 9.01%); IR (KBr): ν_{max}/cm^{-1} 1261 (C–O–C); δ_H (300 MHz, $CDCl_3$) 7.84 (12H, s, ArH), 4.24 (24H, t, OCH_2), 1.89–1.96 (24H, m, OCH_2CH_2), 1.51–1.70 (28H, m, CH_2), 1.05 (30H, t, CH_3); HRMS (ESI): calc. *m*/*z* 1318.8618 ($C_{84}H_{118}O_{12}$), found *m*/*z* 1318.8598 $(M)^+$.

1,9-Bis(3′,6′,7′,10′,11′-pentabutyloxytriphenylen-2′-yloxy)-nonane ***4h*** (0.29 g, 52%): TLC R_f: 0.40 (dichloromethane–hexane 2 : 1); (found: C, 76.57; H, 9.0. $C_{85}H_{120}O_{12}$ requires: C, 76.54; H, 9.07%); IR (KBr): ν_{max}/cm^{-1} 1260 (C–O–C); δ_H (300 MHz, $CDCl_3$) 7.84 (12H, s, ArH), 4.25 (24H, t, OCH_2), 1.83–1.98 (24H, m, OCH_2CH_2), 1.46–1.68 (30H, m, CH_2), 1.05 (30H, t, CH_3); HRMS (ESI): calc. *m*/*z* 1332.8774 ($C_{85}H_{120}O_{12}$), found *m*/*z* 1332.8784 $(M)^+$.

1,10-Bis(3′,6′,7′,10′,11′-pentabutyloxytriphenylen-2′-yloxy)-decane ***4i*** (0.23 g, 42%): TLC R_f: 0.45 (dichloromethane–hexane 2 : 1); (found: C, 76.52; H, 9.09. $C_{86}H_{122}O_{12}$ requires: C, 76.63; H, 9.12%); IR (KBr): ν_{max}/cm^{-1} 1263 (C–O–C); δ_H (300 MHz, $CDCl_3$) 7.85 (12H, s, ArH), 4.25 (24H, t, OCH_2), 1.89–1.98 (24H, m, OCH_2CH_2), 1.26–1.67 (32H, m, CH_2), 1.05 (30H, t, CH_3); HRMS (ESI): calc. *m*/*z* 1346.8931 ($C_{86}H_{122}O_{12}$), found *m*/*z* 1346.8922 $(M)^+$.

1,11-Bis(3′,6′,7′,10′,11′-pentabutyloxytriphenylen-2′-yloxy)-undecane ***4j*** (0.26 g, 47%): TLC R_f: 0.45 (dichloromethane–hexane 2 : 1); (found: C, 76.55; H, 9.15. $C_{87}H_{124}O_{12}$ requires: C, 76.73; H, 9.18%); IR (KBr): ν_{max}/cm^{-1} 1263 (C–O–C); δ_H (300 MHz, $CDCl_3$) 7.84 (12H, s, ArH), 4.25 (24H, t, OCH_2), 1.89–1.96 (24H, m, OCH_2CH_2), 1.23–1.67 (34H, m, CH_2), 1.05 (30H, t, CH_3); HRMS (ESI): calc. *m*/*z* 1360.9087 ($C_{87}H_{124}O_{12}$), found *m*/*z* 1360.9038 $(M)^+$.

1,12-Bis(3′,6′,7′,10′,11′-pentabutyloxytriphenylen-2′-yloxy)-dodecane ***4k*** (0.21 g, 37%): TLC R_f: 0.48 (dichloromethane–hexane 2 : 1); (found: C, 76.54; H, 9.10. $C_{88}H_{126}O_{12}$ requires: C, 76.82; H, 9.23%); IR (KBr): ν_{max}/cm^{-1} 1261 (C–O–C); δ_H (300 MHz, $CDCl_3$) 7.84 (12H, s, ArH), 4.25 (24H, t, OCH_2), 1.89–1.96 (24H, m, OCH_2CH_2), 1.26–1.67 (36H, m, CH_2), 1.05 (30H, t, CH_3); HRMS (ESI): calc. *m*/*z* 1374.9118 ($C_{88}H_{126}O_{12}$), found *m*/*z* 1374.9148 $(M)^+$.

Acknowledgements

This work is supported by the fund from Beijing Natural Science Foundation, China (4122027) and Beijing Municipal Education Commission Project under Grant (no. KM2011 100 15003), the Key (Key grant) Project of Chinese Ministry of Education (no. 211004), Beijing Municipal party committee Organization department project under Grant (no. 2010D0 05004000 006) and The Importation and Development of High-Caliber Talents Project of Beijing Municipal Institutions (CIT&TCD201304123). The authors thank Ao Zhang for helpful discussions.

Notes and references

1 S. Chandrasekhar, B. K. Sadashiva and K. A. Suresh, *Pramana*, 1977, **9**, 471–480.
2 R. J. Bushby and O. R. Lozman, *Curr. Opin. Solid State Mater. Sci.*, 2002, **6**, 569–578.
3 W. Pisula, M. Zorn, J. Y. Chang, K. Müllen and R. Zentel, *Macromol. Rapid Commun.*, 2009, **30**, 1179–1202.
4 J. Hanna, *Opto-Electron. Rev.*, 2005, **13**, 259–267.
5 F. J. M. Hoeben, P. Jonkheijm, E. W. Meijer and A. P. H. J. Schenning, *Chem. Rev.*, 2005, **105**, 1491–1546.
6 Z. An, J. Yu, S. C. Jones, S. Barlow, S. Yoo, B. Domercq, P. Prins, L. D. A. Siebbeles, B. Kippelen and S. R. Marder, *Adv. Mater.*, 2005, **17**, 2580–2583.
7 J. Wu, W. Pisula and K. Müllen, *Chem. Rev.*, 2007, **107**, 718–747.
8 M. O'Neilland and S. M. Kelly, *Adv. Mater.*, 2011, **23**, 566–584.
9 D. Adam, F. Closs, T. Frey, D. Funhoff, D. Haarer, H. Ringsdorf, P. Schuhmacher and K. Siemensmeyer, *Phys. Rev. Lett.*, 1993, **70**, 457–460.
10 D. Adam, P. Schuhmacher, J. Simmerer, L. Haeussling, K. Siemensmeyer, K. H. Etzbach, H. Ringsdorf and D. Haarer, *Nature*, 1994, **371**, 141–143.
11 N. Boden, R. J. Bushby, J. Clements, B. Movaghar, K. J. Fonobsn and T. Kreouzis, *Phys. Rev. B: Condens. Matter Mater. Phys.*, 1995, **52**, 13274–13280.
12 Z. An, J. Yu, B. Domercq, S. C. Jones, S. Barlow, B. Kippelen and S. R. Marder, *J. Mater. Chem.*, 2009, **19**, 6688–6698.
13 J. Simmerer, B. Glüsen, W. Paulus, A. Kettner, P. Schuhmacher, D. Adam, K. H. Etzbach, K. Siemensmeyer, J. H. Wendorff, H. Ringsdorf and D. Haarer, *Adv. Mater.*, 1996, **8**, 815–819.
14 A. M. van de Craats, J. M. Warman, A. Fechtenkötter, J. D. Brand, M. A. Harbison and K. Müllen, *Adv. Mater.*, 1999, **11**, 1469–1472.
15 A. Ochse, A. Kettner, J. Kopitzke, J. H. Wendorff and H. Bassler, *Phys. Chem. Chem. Phys.*, 1999, **1**, 1757–1760.
16 B. Glüsen, W. Heitz, A. Kettner and J. H. Wendorff, *Liq. Cryst.*, 1996, **20**, 627–633.
17 B. Glüsen, A. Kettner and J. H. Wendorff, *Mol. Cryst. Liq. Cryst.*, 1997, **303**, 115–120.
18 P. G. Schouten, J. M. Warman, M. P. de Haas, C. F. van Nostrum, G. H. Gelinck, R. J. M. Nolte, M. J. Copyn, J. W. Zwikker, M. K. Engel, M. Hanack, Y. H. Chang and W. T. Ford, *J. Am. Chem. Soc.*, 1994, **116**, 6880–6894.
19 A. M. van de Craats, J. M. Warman, M. P. de Haas, D. Adam, J. Simmerer, D. Haarer and P. Schuhmacher, *Adv. Mater.*, 1996, **8**, 823–826.
20 S. Kumar, *Liq. Cryst.*, 2005, **32**, 1089–1113.
21 N. Boden, R. J. Bushby, A. N. Cammidge, A. E. Mansoury, P. S. Martin and Z. Lu, *J. Mater. Chem.*, 1999, **9**, 1391–1402.
22 N. Boden, R. C. Borner, R. J. Bushby, A. N. Carnmidge and M. V. Jesudason, *Liq. Cryst.*, 1993, **15**, 851.
23 S. Kumar and M. Manickam, *Synthesis*, 1998, **8**, 1119–1122.
24 D. Adam, P. Schuhmacher, J. Simmerer, L. Häussling, W. Paulus, K. Siemensmeyer, K. H. Etzbach, H. Ringsdorf and D. Haarer, *Adv. Mater.*, 1995, **7**, 276–280.
25 G. C. Bryant, M. J. Cook, S. O. Haslam, R. M. Richardson, T. G. Ryan and A. J. Thorne, *J. Mater. Chem.*, 1994, **4**, 209–216.

26 S. Laschat, A. Baro, N. Steinke, F. Giesselmann, C. Hägele, G. Scalia, R. Judele, E. Kapatsina, S. Sauer, A. Schreivogel and M. Tosoni, *Angew. Chem., Int. Ed.*, 2007, **46**, 4832–4887.
27 V. De Cupere, J. Tant, P. Viville, R. Lazzaroni, W. Osikowicz, W. R. Salaneck and Y. H. Geerts, *Langmuir*, 2006, **22**, 7798–7806.
28 I. Dierking, *Textures of Liquid Crystals*, Wiley-VCH, Weinheim, 2003.
29 B. Glüsen, A. Kettner, J. Kopitzke and J. H. Wendorff, *J. Non-Cryst. Solids*, 1998, **241**, 113–120.
30 F. C. Frank and S. Chandrasekhar, *J. Phys.*, 1980, **41**, 1285–1288.
31 A. M. Levelut, *J. Chim. Phys. Phys.-Chim. Biol.*, 1983, **80**, 149–161.
32 F. Morale, R. W. Date, D. Guillon, D. W. Bruce, R. L. Finn, C. Wilson, A. J. Blake, M. Schröder and B. Donnio, *Chem.–Eur. J.*, 2003, **9**, 2484–2501.
33 J. Q. Jiang, Z. R. Shen, J. Lu, P. F. Fu, Y. Lin, H. D. Tang, H. W. Gu, J. Sun, P. Xie and R. B. Zhang, *Adv. Mater.*, 2004, **16**, 1534–1539.
34 K. Kishikawa, S. Nakahara, Y. Nishikawa, S. Kohmoto and M. Yamamoto, *J. Am. Chem. Soc.*, 2005, **127**, 2565–2571.
35 E. J. Foster, C. Lavigueur, Y.-C. Ke and V. E. Williams, *J. Mater. Chem.*, 2005, **15**, 4062–4068.
36 H. Zheng, C. K. Lai and T. M. Swager, *Chem. Mater.*, 1996, **7**, 2067–2077.
37 C. P. Lillya and Y. L. N. Murthy, *Mol. Cryst. Liq. Cryst., Lett. Sect.*, 1985, **2**, 121–125.
38 S. Zamir, E. J. Wachtel, H. Zimmermann, S. Dai, N. Spielberg, R. Poupko and Z. Luz, *Liq. Cryst.*, 1997, **23**, 689–698.
39 S. J. Mahoney, M. M. Ahmida, H. Kayal, N. Fox, Y. Shimizu and S. H. Eichhorn, *J. Mater. Chem.*, 2009, **19**, 9221–9232.